IEEE Photonics Journal
An IEEE Photonics Society Publication

Open Access

# Influence of the Dielectric PMMA Layer on the Detectivity of Pentacene-Based Photodetector With Field-Effect Transistor Configuration in Visible Region

Volume 5, Number 6, December 2013

D. Yang
L. Zhang
S. Y. Yang
B. S. Zou

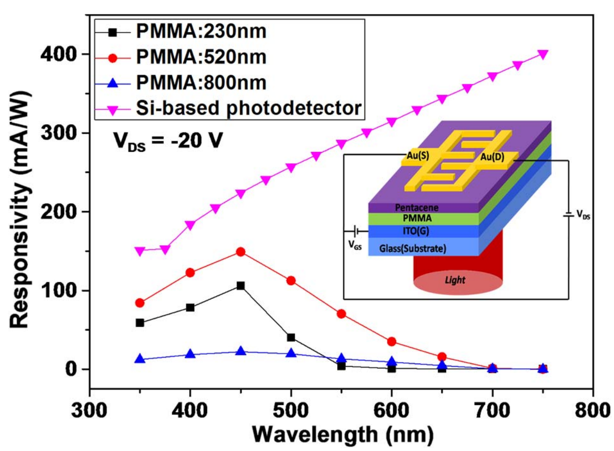


DOI: 10.1109/JPHOT.2013.2293616
1943-0655 

# Influence of the Dielectric PMMA Layer on the Detectivity of Pentacene-Based Photodetector With Field-Effect Transistor Configuration in Visible Region

**D. Yang, L. Zhang, S. Y. Yang, and B. S. Zou**

Beijing Key Lab of Nanophotonics and Ultrafine Optoelectronic Systems, School of Physics, Beijing Institute of Technology, Beijing 100081, China

*DOI: 10.1109/JPHOT.2013.2293616*


Manuscript received October 8, 2013; revised November 12, 2013; accepted November 21, 2013. Date of publication December 5, 2013; date of current version December 11, 2013. This work was supported in part by the National Natural Science Foundation of China under Grant 60777025, by the Cooperation Project of Beijing Nova Program (XXHZ201204), by the Foundation of Distinguished Teacher (BIT-JC-201005) and the "111" Research Base (BIT111-201101) at Beijing Institute of Technology (BIT), and by the program from the Key Laboratory of Photoelectronic Imaging Technology and System (2012OEIOF02), BIT, Ministry of Education of China. Corresponding author: S. Y. Yang (e-mail: syyang@bit.edu.cn).

**Abstract:** In this paper, the influence of dielectric polymethylmethacrylate (PMMA) layer on the detectivity of pentacene-based photodetectors with field-effect transistor (FET) configuration were investigated in a visible region. By changing the thickness of the PMMA layer, from 230 nm to 520 nm and 800 nm, electrical parameters, such as the capacitance, "on/off" current ratio, and carrier mobility, of the pentacene-based photodetector decrease with increasing the thickness of the PMMA layer, which influences its detectivity directly. The photosensitivity and responsivity of the FET-based pentacene photodetector with 520-nm PMMA varied with incident monochromatic light from 350 nm to 750 nm, and it showed a maximum responsivity of 149 mA/W with a photosensitivity peak of $1.7 \times 10^4$ at 450 nm, which is of the same order as that of the standard Si-based photodetector. Therefore, it is an applicable way to get such kind of FET-based full-organic photodetectors in a full visible region with excellent photosensitivity, responsivity, and selectivity.

**Index Terms:** Organic photodetectors, organic field-effect transistor (OFET), photosensitivity, responsivity.

## 1. Introduction

The influence of light on organic field-effect transistors (OFETs) has attracted extensive attention in theoretical researches [1], [2] and practical applications [3]–[5] since its first report in 2001 [6]. Due to the advantages of organic semiconductors (OSCs), such as easy preparation, low cost, light weight, and compatibility with soft substrates, researchers combined the photoconductive effect of OSCs with the field effect of OFETs to fabricate field-effect transistor (FET)-based photodetectors [7]–[10] with excellent photosensitive properties and easy integration into electronic circuits. Different from common photodetectors like photodiodes, FET-based photodetectors overcome the shortcomings of exciton quenching and low optical gain through an electrical gate bias, which is used to modulate the lateral field across the active layer between source and drain electrodes. This electric field causes the separation of photogenerated carriers and greatly extends the carrier recombination lifetime, leading to a much higher sensitivity and lower noise.

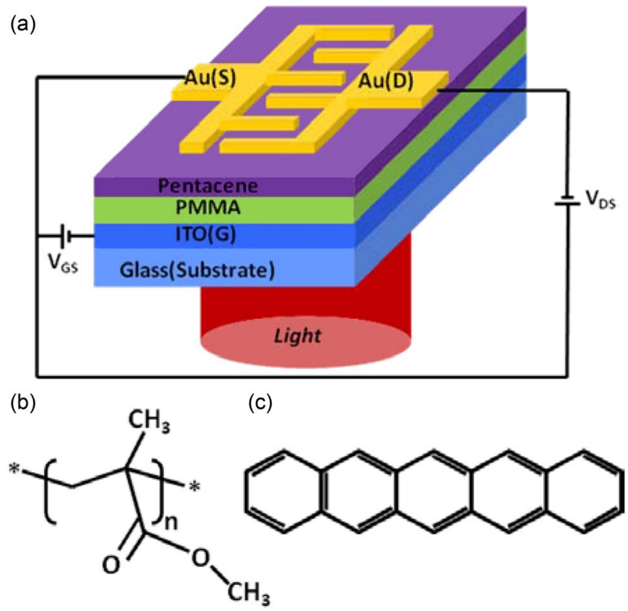


Fig. 1. (a) Configuration of FET-based pentacene photodetector and the molecular structures of (b) PMMA and (c) pentacene.

A wide variety of OSCs, such as small molecules [8]–[12], polymer OSCs [13], [14], and blended OSCs [15], [16], have shown their high photosensitive property in OFET. Among these OSCs, pentacene with high air stability, high carrier mobility, and "on/off" current ratio $(I_{on}/I_{off})$ has exhibited highly electrical and photosensitive characteristics, and it is an ideal candidate as the active layer in the organic photodetector with FET configuration [8]–[10], [17]. Some reports on pentacene-based OFETs have pointed out that many factors can affect the photosensitive properties, and these factors include the exciton lifetime [18], the intensity or wavelength of the incident light [9], and the surface roughness or thickness of pentacene layer [19]. Also, a highly sensitive photodetector is an essential element in image sensors. Therefore, in this contribution, we fabricated pentacene-based photodetectors with FET configuration and investigated the influence of the dielectric layer thickness on the detectivity in the full visible region, and it provides a method for fabricating full-organic image sensors.

In our experiments, pentacene was chosen as the active layer due to its excellent field-effect characteristics and high absorbance in the full visible region. In order to realize the detection, solution-processed polymethylmethacrylate (PMMA) was selected as the dielectric layer due to its well transparency, dielectricity, film-forming property, simple process, and low cost [20], [21]. In the full visible region, different monochromatic lights from 350 nm to 750 nm were chosen as incident light to illuminate pentacene-based photodetectors with FET configuration, and we found that the photosensitivity and responsivity of these organic photodetectors vary with the PMMA thicknesses and incident wavelengths. Having good performance as that of the standard Si-based photodetector, the FET-based pentacene photodetectors show excellent detectivity and selectivity in the full visible region.

## 2. Experimental Setup

Fig. 1 shows the diagram of bottom-gate/top-contact (BGTC) FET-based pentacene photodetector and the molecular structures of materials used in our experiments. First, patterned ITO/glass substrates (from ShenZhen Nanbo Group) were cleaned successively with deionized water, acetone, and ethanol in ultrasonic bath and then by ozone treatment for 2 min. In order to investigate the effect of the dielectric layer thickness on device performance, PMMA (Alfa-Aesar, MW $=$ 120 000) was dissolved in toluene with a series of concentrations of 40 mg/mL, 60 mg/mL, and 80 mg/mL, respectively, and then, it was spin-coated on the ITO substrate at 2000 rpm in the nitrogen-filled glove box. After annealing treatment of PMMA film at 100 °C for 60 min, 35 nm pentacene (Sigma-Aldrich, 99% in purity) film was thermally evaporated on it in a vacuum of $2 \times 10^4$ Pa at a rate of 0.01–0.03 nm/s. Finally, 50 nm gold drain and source electrodes were fabricated by thermal evaporation through a shadow mask. The effective area of our photodetector is $2 \times 2$ mm$^2$. The channel length and channel width are 100 $\mu$m and 17.2 mm, respectively. The transmissivity of ITO is more than 85% in the visible region.

The thickness and capacitance of the dielectric layer were measured with an XP-2 high resolution surface profiler and a precision LCR meter (Fluke PM6304), respectively. The absorption spectrum of the pentacene film was measured with a UV-vis double beam spectrophotometer (Mapada UV-6100). The current-voltage $(I\text{-}V)$ characteristics of the devices were recorded using a Keithley semiconductor characterization system (Model 4200-SCS). The full-spectrum visible light was supplied by a simulated sunlight test system (7-SCSpec). A xenon lamp with optical interference filters and neutral density filters was used as the light source, which permits the incident monochromatic wavelength to be selected from 350 nm to 750 nm from the bottom of the devices, as shown in Fig. 1. All the measurements were done in ambient air at room temperature.

## 3. Results and Discussion

### 3.1. Electrical Parameters of Photodetectors

To investigate the influence of the dielectric layer thickness on the FET-based organic photodetectors, we fabricated three devices with PMMA thickness of 230 nm, 520 nm, and 800 nm, respectively. The capacitance of the dielectric layer varies with its thickness, which determines the electrical property of the device. The capacitances of PMMA dielectric layers are 11.21 nF/cm$^2$, 5.16 nF/cm$^2$, and 3.23 nF/cm$^2$ for 230 nm, 520 nm, and 800 nm PMMA layers, respectively, by measuring with a parallel plate capacitor structure (ITO/PMMA/Au) at the frequency of 100 kHz.

Fig. 2 shows the output and transfer characteristics of FET-based pentacene photodetectors. In Fig. 2(a), (c), and (e), the linear and saturation regions of all the devices can be observed clearly with increasing negative gate voltages, exhibiting a typical p-channel accumulation-type FET behavior. At lower voltages, drain-source current-voltage ($I_{DS}-V_{DS}$) curves exhibit good linearity. This confirms that a good ohmic contact was established between the pentacene and gold electrodes [22]. It can be seen that thinner dielectric layer exhibits higher saturation current and larger $I_{\text{on}}/I_{\text{off}}$, and the highest $I_{\text{on}}/I_{\text{off}}$ of $10^6$ is obtained at 230 nm because the capacity for storing charges decreases with increasing the thickness of the dielectric layer.

From the transfer characteristics in Fig. 2(b), (d), and (f), one can see that $I_{DS}$ decreases by two orders of magnitude and the threshold voltage $(V_{\text{th}})$ increases from $-10.2$ V to $-15.7$ V as the thickness of the dielectric layer increases from 230 nm to 800 nm. The $V_{\text{th}}$ value is determined by the intercept of the $(|I_{DS}|^{1/2} - V_{GS})$ plot. The carrier mobility $(\mu)$ is obtained from the saturation regime by the following Eq. (1) [23]:

$$I_{DS} = \frac{W}{2L} C_i \mu (V_{GS} - V_{\text{th}})^2 \tag{1}$$

where $C_i$ is the capacitance per unit area of the dielectric layer, and $W$ and $L$ are the channel width and the channel length, respectively. The carrier mobility of the photodetector with 230 nm PMMA is 0.31 cm$^2$/V $\cdot$ s, which is higher than others. Whereas the current at "off" state is large due to the thin dielectric layer, which is unfavorable to obtain good detectivity. The current at "off" state for photodetector with 800 nm PMMA is small, but its low carrier mobility of 0.04 cm$^2$/V $\cdot$ s may also limit its detectivity. Therefore, the photodetector with 520 nm PMMA may have good detectivity, which exhibits appropriate carrier mobility and current density at "off" state. All electrical parameters of FET-based organic photodetectors were summarized in Table 1.

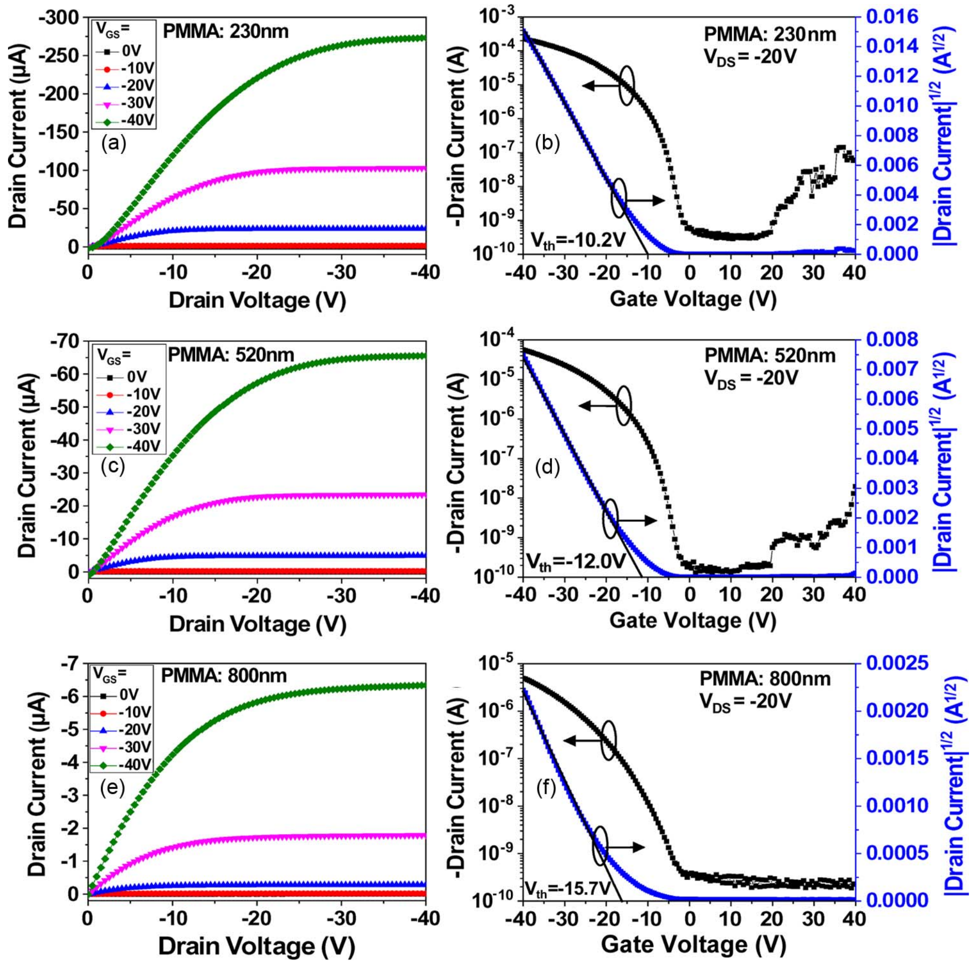


Fig. 2. Output and transfer characteristics of FET-based pentacene photodetectors with different thicknesses of PMMA layer: 230 nm [(a) and (b)], 520 nm [(c) and (d)], and 800 nm [(e) and (f)].

TABLE 1

Electrical parameters of FET-based pentacene photodetectors with different PMMA thicknesses

| FET-based photodetectors | Capacitance ($C_i$, nF/ cm$^2$) | "On/off" current ratio ($I_{on}$ /$I_{off}$) | Threshold voltage ($V_{th}$, V) | Carrier mobility (μ, cm$^2$/V s) |
|---|---|---|---|---|
| **PMMA-230 nm** | 11.21 | $10^6$ | -10.2 | 0.31 |
| **PMMA-520 nm** | 5.16 | $10^5$ | -12.0 | 0.19 |
| **PMMA-800 nm** | 3.23 | $10^4$ | -15.7 | 0.04 |

### *3.2. Detecting Parameters of Photodetectors*

To investigate the detectivity of pentacene-based photodetectors with FET configuration, the output and transfer characteristics of the devices were measured under different incident monochromatic light from 350 nm to 750 nm. As shown in Fig. 3(a)–(c), the transfer characteristic curves of the devices move toward the positive voltage with the incident wavelength ($\lambda$) decreasing from

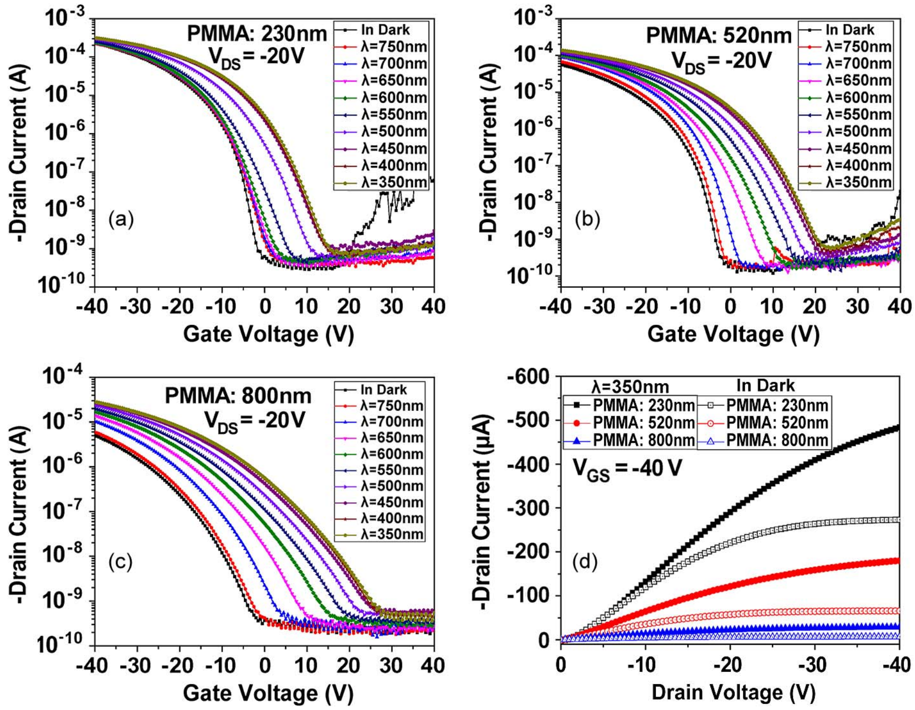


Fig. 3. Transfer characteristics of FET-based pentacene photodetectors with different PMMA thicknesses (a) 230 nm, (b) 520 nm, and (c) 800 nm, measured in dark and under illumination, and (d) output characteristics of these photodetectors in dark and under 350 nm incident light.

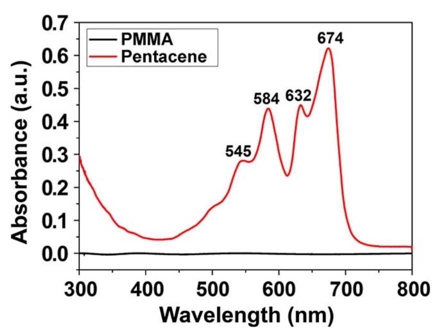


Fig. 4. Absorption spectra of PMMA film (520 nm) and pentacene film (35 nm).

750 nm to 350 nm at $V_{DS} = -20$ V (in the linear region). We also measured the transfer characteristics in the saturation region at $V_{DS} = -40$ V, which had the similar performance as that at $V_{DS} = -20$ V. Keeping at the same $V_{DS}$ and $V_{GS}$ as that in dark, the current at "off" state increases, but $V_{\text{th}}$ decreases with $\lambda$ under illumination, which is due to the photovoltaic effect [24]. Generally speaking, as soon as light with photon energy equal to or higher than the bandgap energy of pentacene is absorbed, a number of photogenerated carriers are formed, and it leads to an increase in $I_{DS}$ and an "on" state of the device. This amplified current can directly reflect the information of incident light. From the absorption spectra of PMMA film (520 nm) and pentacene film (35 nm) (see Fig. 4), one can see that PMMA film shows little absorption as compared with that of pentacene film in visible region. Pentacene film has four absorption peaks of $\pi$ bands at 674 nm, 632 nm, 584 nm, and 545 nm [25], and the optical bandgap is around 700 nm. In our experiments, organic photodetectors generated a tiny photocurrent under 750 nm monochromatic light, which is

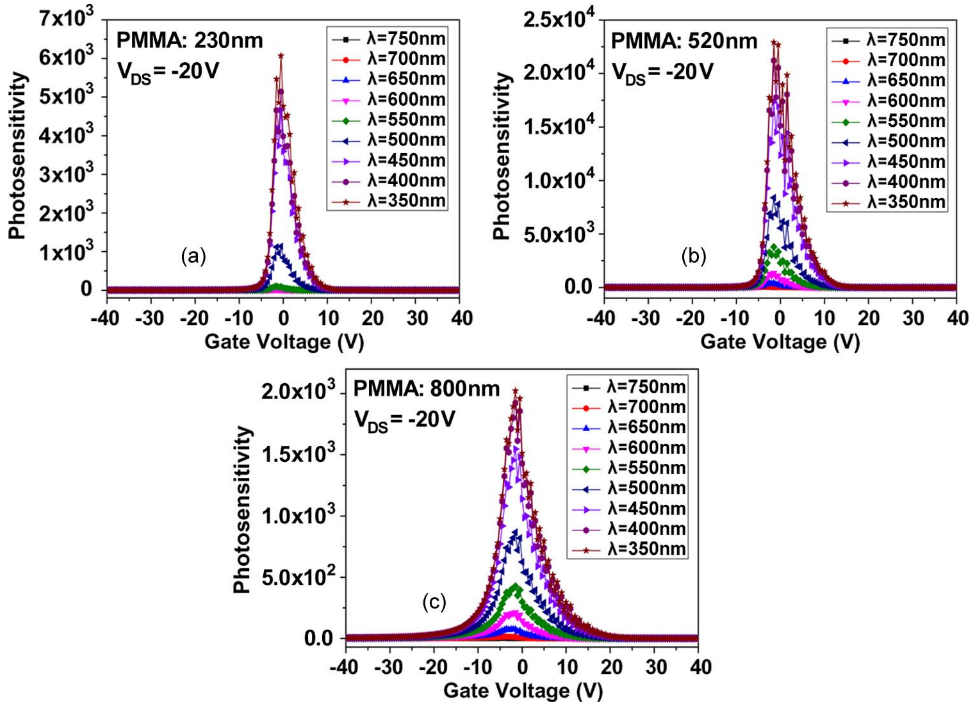


Fig. 5. Photosensitivity as a function of the gate voltage under monochromatic light at $V_{DS} = -20$ V by varying the incident wavelength from 750 nm to 350 nm. Here, FET-based pentacene photodetectors are with different PMMA dielectric layer: (a) 230 nm, (b) 520 nm, and (c) 800 nm.

due to the defects and impurities at the interface of pentacene/PMMA. Being illuminated with incident wavelength from 700 nm to 350 nm, organic photodetectors generated more and more photo-induced carriers to increase $I_{DS}$, and the biggest change can also be observed clearly in the output characteristics of these three photodetectors in dark and under 350 nm incident light at $V_{GS} = -40$ V, as shown in Fig. 3(d).

For FET-based organic photodetectors, in addition to the normal electrical parameters as that of FETs, the photosensitivity $(P)$ and responsivity $(R)$ are the other two main detecting parameters which determine the detectivity of photodetectors. Photosensitivity is defined by the following Eq. (2) [10]:

$$P = \frac{I_{\rm ph}}{I_{\rm dark}} = \frac{I_{\rm illum} - I_{\rm dark}}{I_{\rm dark}} \tag{2}$$

where $I_{\rm ph}$ is the photocurrent density, and $I_{\rm illum}$ and $I_{\rm dark}$ are the drain-source current under illumination and in the dark, respectively. Normally, we use $I_{\rm ph}/I_{\rm dark}$ to define the photosensitivity. Based on Eq. (2), the $I_{\rm ph}/I_{\rm dark}$ values of photodetectors with PMMA layer of 230 nm, 520 nm, and 800 nm under light at $V_{DS} = -20$ V can be figured out, and they are shown in Fig. 5. $I_{\rm ph}/I_{\rm dark}$ increases with decreasing the incident wavelengths, and the maximum values of these three photodetectors are $6.0 \times 10^3$, $2.3 \times 10^4$, and $2.0 \times 10^3$ under 350 nm light, respectively. These results are consistent with our prediction above. Small current at "off" state appears in the FET-based pentacene photodetector with thick dielectric layer, which is favorable to obtain high detectivity. At the same time, however, the detectivity is also limited by the low carrier mobility of the photodetector with thick PMMA layer. Considering the small current at "off" state and the high carrier mobility comprehensively, appropriate thickness of the dielectric layer is desired, and the photodetector with 520 nm PMMA has a larger $I_{\rm ph}/I_{\rm dark}$ than the other two. Fig. 5 shows the characteristics of $I_{\rm ph}/I_{\rm dark}$ as a function of the gate voltage $(V_{GS})$ under different monochromatic light, which indicates $V_{GS}$

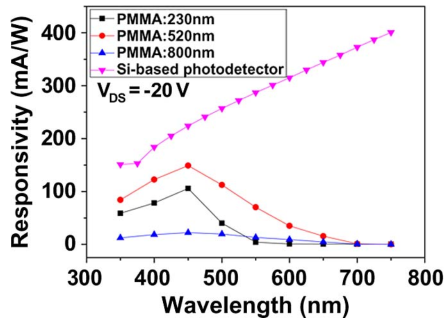


Fig. 6. Responsivities of FET-based pentacene photodetectors with different PMMA thicknesses and the standard Si-based photodetector as the function of the incident wavelength at $V_{DS} = -20$ V.

has an obvious modulation effect on $I_{ph}/I_{dark}$. The maximum $I_{ph}/I_{dark}$ appears at "off" state ($V_{GS} \sim 0$ V), and it is much higher than that at "on" state ($V_{GS} = -40$ V). The reason is that the conductivity at "on" state is mainly dominated by the field-induced charges, whereas the device is charge-depleted at "off" state and only the photocurrent contributes to $I_{DS}$ [26]. For a certain incident monochromatic light, $I_{ph}/I_{dark}$ changes with increasing $V_{GS}$ from $-40$ V to 40 V, and the peak of $I_{ph}/I_{dark}$ appears at the same $V_{GS}$ even under different monochromatic lights. The $I_{ph}/I_{dark}$ values under monochromatic light at different $V_{DS}$ were also figured out, and it demonstrates that the maximum $I_{ph}/I_{dark}$ values appear at the same $V_{GS}$. Therefore, one can see that the modulation effect of $V_{GS}$ on $I_{ph}/I_{dark}$ is independent of incident wavelength $\lambda$ and $V_{DS}$. Certainly, FET-based pentacene photodetectors can reach higher $I_{ph}/I_{dark}$ values at "off" state by controlling $V_{GS}$.

Another important parameter of photodetector, responsivity, reveals the extent of the incident optical power being changed into the current, which is usually expressed as Eq. (3) [10], i.e.,

$$R = \frac{I_{ph}}{P_{inc}} = \frac{I_{illum} - I_{dark}}{E_{inc} \times A} \quad (3)$$

where $P_{inc}$ is the incident illumination power on the photodetector, which can be written as the product of the incident illumination irradiance $E_{inc}$ and the effective area $A$ of the photodetector. In our experiments, we chose a standard Si-based photodetector as a reference to detect the same light, of which the responsivity ($R_{Si}$), photocurrent ($I_{phSi}$), and effective area ($A_{Si}$) are known. Therefore, the responsivity ($R$) of our organic photodetector under incident light can be figured out by the following Eq. (4):

$$R(\lambda) = R_{Si}(\lambda)\frac{I_{ph}(\lambda)A_{Si}}{I_{phSi}(\lambda)A} \quad (4)$$

where $I_{ph}$ is the maximum photocurrent of our photodetector for a certain incident wavelength. Fig. 6 shows the responsivities of photodetectors with different PMMA thicknesses and of the standard Si-based photodetector versus incident wavelength $\lambda$. For all these devices, there is no response when $\lambda$ is higher than the threshold wavelength of 700 nm. The responsivity increases first and then decreases with reducing incident wavelength $\lambda$. We have noted that the responsivity was not too high when its absorption coefficient was large in the long wavelength region, and this similar phenomenon has been explained by the internal filter effect [27]. Light with a large absorption coefficient is filtered in the pentacene film by absorption and does not contribute to generate the current. In addition, we think there should be other reasons, such as the thin pentacene film and illumination from the bottom of the device in our experiments, responsible to the phenomenon. As shown in Fig. 4, one can see that the absorption peaks at 674 nm and 632 nm originate the Davydov doublet of the 0-0 band and the other two peaks at 584 nm and 545 nm originate the Davydov doublet of the 0-1 band [28], and they all belong to the transitions of organic molecular vibronic states. Most of the absorption energy radiates in some ways and makes little contribution to the formation of photogenerated carriers, so we only obtain low responsivities from the tiny amplified current. Under illumination of 450 nm incident light, the maximum responsivity of photodetectors with 230 nm, 520 nm, and 800 nm PMMA are 106 mA/W, 149 mA/W, and 22 mA/W, and the corresponding $I_{ph}/I_{dark}$ peak values are $4.7 \times 10^3$, $1.7 \times 10^4$, and $1.5 \times 10^3$, respectively. Due to the larger photocurrent, the photodetector with 520 nm PMMA shows a higher responsivity than the other two, which is of the same order as the standard Si-based photodetector. Therefore, it is promising for such a kind of FET-based organic photodetector to be used as a visible light photodetector with excellent photosensitivity, responsivity, and light selectivity in the near future.

## 4. Conclusion

In conclusion, we have successfully demonstrated high-performance pentacene-based photodetectors with FET configuration. Except for $V_{th}$, both $I_{on}/I_{off}$ and carrier mobility of the photodetectors decrease with increasing the thickness of PMMA from 230 nm to 520 nm and 800 nm, and the reduction of current at "off" state is beneficial to obtain high $I_{ph}/I_{dark}$ and responsivity. Under illumination, $I_{DS}$ was amplified and increased with reducing incident wavelength, which made the photodetector shift from "off" state to "on" state. $V_{GS}$ had obvious modulation effect on $I_{ph}/I_{dark}$ of the photodetector, which was independent of incident wavelength and $V_{DS}$. The photodetector with 520 nm PMMA showed a maximum responsivity of 149 mA/W under 450 nm monochromatic light at $V_{DS} = -20$ V. Therefore, after further configuration optimization, such a kind of FET-based pentacene photodetector may be used as a visible light photodetector due to its excellent photosensitivity, responsivity, and selectivity.

## References


[1] S. Dutta and K. S. Narayan, "Nonexponential relaxation of photoinduced conductance in organic field-effect transistors," *Phys. Rev. B, Condens. Matter*, vol. 68, no. 12, pp. 125208-1–125208-4, Sep. 2003.

[2] M. Debucquoy, S. Verlaak, S. Steudel, K. Myny, J. Genoe, and P. Heremans, "Correlation between bias stress instability and phototransistor operation of pentacene thin-film transistors," *Appl. Phys. Lett.*, vol. 91, no. 10, pp. 103508-1–103508-3, Sep. 2007.

[3] T. D. Anthopoulos, "Electro-optical circuits based on light-sensing ambipolar organic field-effect transistors," *Appl. Phys. Lett.*, vol. 91, no. 11, pp. 113513-1–113513-3, Sep. 2007.

[4] Y. L. Guo, C. A. Di, S. H. Ye, X. N. Sun, J. Zheng, Y. G. Wen, W. P. Wu, G. Yu, and Y. Q. Liu, "Multibit storage of organic thin-film field-effect transistors," *Adv. Mater.*, vol. 21, no. 19, pp. 1954–1959, May 2009.

[5] B. Mukherjee, M. Mukherjee, Y. Choi, and S. Pyo, "Control over multifunctionality in optoelectronic device based on organic phototransistor," *ACS Appl. Mater. Interfaces*, vol. 2, no. 6, pp. 1614–1620, Jun. 2010.

[6] K. S. Narayan and N. Kumar, "Light responsive polymer field-effect transistor," *Appl. Phys. Lett.*, vol. 79, no. 12, pp. 1891–1893, Sep. 2001.

[7] S. Y. Yang, N. Zhao, L. Zhang, H. Z. Zhong, R. B. Liu, and B. S. Zou, "Field-effect transistor-based solution-processed colloidal quantum dot photodetector with broad bandwidth into near-infrared region," *Nanotechnol.*, vol. 23, no. 25, pp. 255203-1–255203-6, Jun. 2012.

[8] I. Kymissis, C. G. Sodini, A. I. Akinwande, and V. Bulovi, "An organic semiconductor based process for photodetecting applications," in *IEDM Tech. Dig.*, 2004, pp. 377–380.

[9] Y. Y. Noh and D. Y. Kim, "Organic phototransistor based on pentacene as an efficient red light sensor," *Solid-State Electron.*, vol. 51, no. 7, pp. 1052–1055, Jul. 2007.

[10] M. C. Hamilton and J. Kanicki, "Organic polymer thin-film transistor photosensors," *IEEE J. Sel. Topics Quantum Electron.*, vol. 10, no. 4, pp. 840–848, Jul./Aug. 2004.

[11] M. Y. Cho, S. J. Kim, Y. D. Han, D. H. Park, K. H. Kim, D. H. Choi, and J. Joo, "Highly sensitive, photocontrolled, organic thin-film transistors using soluble star-shaped conjugated molecules," *Adv. Funct. Mater.*, vol. 18, no. 19, pp. 2905–2912, Oct. 2008.

[12] B. Mukherjee, M. Mukherjee, Y. Choi, and S. Pyo, "Organic phototransistor with n-type semiconductor channel and polymeric gate dielectric," *J. Phys. Chem. C*, vol. 113, no. 43, pp. 18 870–18 873, Oct. 2009.

[13] H. L. Dong, H. X. Li, E. J. Wang, H. Nakashima, K. Torimitsu, and W. P. Hu, "Phototransistors of a rigid rod conjugated polymer," *J. Phys. Chem. C*, vol. 112, no. 49, pp. 19 690–19 693, Dec. 2008.

[14] K. Wasapinyokul, W. I. Milne, and D. P. Chu, "Photoresponse and saturation behavior of organic thin film transistors," *J. Appl. Phys.*, vol. 105, no. 2, pp. 024509-1–024509-8, Jan. 2009.

[15] N. Marjanovi, T. B. Singh, G. Dennler, S. Günes, H. Neugebauer, N. S. Sariciftci, R. Schwödiauer, and S. Bauer, "Photoresponse of organic field-effect transistors based on conjugated polymer/fullerene blends," *Org. Electron.*, vol. 7, no. 4, pp. 188–194, Aug. 2006.

[16] S. M. Mok, F. Yan, and H. L. W. Chan, "Organic phototransistor based on poly (3-hexylthiophene)/TiO2 nanoparticle composite," *Appl. Phys. Lett.*, vol. 93, no. 2, pp. 023310-1–023310-3, Jul. 2008.

[17] H. W. Zan, W. W. Tsai, Y. R. Lo, Y. M. Wu, and Y. S. Yang, “Pentacene-based organic thin film transistors for ammonia sensing,” *IEEE Sensors J.*, vol. 12, no. 3, pp. 594–601, Mar. 2012.
[18] M. Debucquoy, S. Verlaak, S. Stoedel, S. D. Vusser, J. Genoe, and P. Heremans, “Pentacene organic field-effect phototransistor with memory-effect,” in *Proc. SPIE*, 2006, pp. 61921F-1–61921F-10.
[19] A. E. Amrani, B. Lucas, and B. Ratier, “The effect of the active layer thickness on the performance of pentacene-based phototransistors,” *Synthetic Metals*, vol. 161, no. 23/24, pp. 2566–2569, Jan. 2012.
[20] J. Veres, S. Ogier, and G. Lloyd, “Gate insulators in organic field-effect transistors,” *Chem. Mater.*, vol. 16, no. 23, pp. 4543–4555, Nov. 2004.
[21] Y. J. Yun, C. Pearson, and M. C. Petty, “Pentacene thin film transistors with a poly (methyl methacrylate) gate dielectric: Optimization of device performance,” *J. Appl. Phys.*, vol. 105, no. 3, pp. 034508-1–034508-7, Feb. 2009.
[22] S. Okur, F. Yakuphanoglu, and E. Stathatos, “High-mobility pentacene phototransistor with nanostructured $SiO_2$ gate dielectric synthesized by sol-gel method,” *Microelectron. Eng.*, vol. 87, no. 4, pp. 635–640, Apr. 2010.
[23] Y. L. Guo, G. Yu, and Y. Q. Liu, “Functional organic field-effect transistors,” *Adv. Mater.*, vol. 22, no. 40, pp. 4427–4447, Oct. 2010.
[24] H. S. Kang, C. S. Choi, W. Y. Choi, D. H. Kim, and K. S. Seo, “Characterization of phototransistor internal gain in metamorphic high-electron-mobility transistors,” *Appl. Phys. Lett.*, vol. 84, no. 19, pp. 3780–3782, May 2004.
[25] T. Minakata, I. Nagoya, and M. Ozaki, “Highly ordered and conducting thin film of pentacene doped with iodine vapor,” *J. Appl. Phys.*, vol. 69, no. 10, pp. 7354–7356, May 1991.
[26] M. M. Torrent, P. Hadley, N. Crivillers, J. Veciana, and C. Rovira, “Large photoresponsivity in high-mobility single-crystal organic field-effect phototransistors,” *Chem. Phys. Chem.*, vol. 7, no. 1, pp. 86–88, Jan. 2006.
[27] Y. Y. Noh, D. Y. Kim, and K. Yase, “Highly sensitive thin-film organic phototransistors: Effect of wavelength of light source on device performance,” *J. Appl. Phys.*, vol. 98, no. 7, pp. 074505-1–074505-7, Oct. 2005.
[28] Q. Miao, T. Q. Nguyen, T. Someya, G. B. Blanchet, and C. Nuckolls, “Synthesis, assembly, and thin film transistors of dihydrodiazapentacene: An isostructural motif for pentacene,” *J. Amer. Chem. Soc.*, vol. 125, no. 34, pp. 10 284–10 287, Aug. 2003.